Progress In Electromagnetics Research B, Vol. 79, 65–81, 2017

Harmonically Time Varying, Traveling Electromagnetic Fields along a Laminate Approximated by a Homogeneous, Anisotropic Block with Infinite Length

Birger Marcusson* **and Urban Lundin**

Abstract—Analytical expressions that include arbitrarily directed fields on all laminate boundaries can be used for calculation of the fields inside the laminate when the boundary fields are known from, e.g., measurements. A linear laminate block could be used in non-destructive testing for comparisons between different laminates. This article contains derivation of Fourier series of harmonically time varying, traveling electromagnetic fields in homogeneous, anisotropic approximations of laminates. The component of the magnetic field strength in the stacking direction is used as a source term in two-dimensional Poisson equations for the magnetic field strength in other directions. This approximation is here used in three dimensions under the precondition that the conductivity is much smaller in the laminate stacking direction than in the other directions. Sine interpolation and different choices of types of boundary conditions are discussed. Different alternative subdivisions of the Poisson boundary value problems are treated. Shorted derivations of simple analytical expressions are given for both traveling and standing waves in two dimensions. Results from Fourier series in the three-dimensional case are compared with results from finite element calculations.

1. INTRODUCTION

For a simple geometry like an infinitely long laminate block, analytical expressions of the electromagnetic fields combined with measured boundary fields can be used as an alternative to analyses with numerical softwares, such as finite element programs. The analytical expressions can therefore also be used during verification of numerical softwares. Another application of the analytical expressions could be field calculation as a complement to non-destructive testing with sweeping electromagnetic fields for comparisons between laminates. Such tests can be of special interest for laminate plates intended to be located in the end regions of electric machines and plate packages where the eddy current losses are relatively large because of magnetic leakage fields. Sweeping field tests would complement the IEC 60404-2 standard Epstein frame tests since the latter use alternating magnetic fields with a negligible component perpendicular to the lamination planes. The main purpose of this work is to find mathematical expressions for traveling magnetic and electric field components for a laminate approximated by a homogeneous, anisotropic block. To approximate a laminate by a single, homogeneous, anisotropic piece of material is common in finite element analyses (FEA) of electric machines with a magnetic core [1]. The anisotropic approximation can to a high extent reduce the amount of calculations by analytical expressions as well as by FEA since there can be up to a few thousand lamination layers of electrical steel in a core. With the laminate approximated by a homogeneous block, it is sufficient to measure or calculate spatial averages of the boundary fields in

Received 17 August 2017, Accepted 18 October 2017, Scheduled 30 October 2017
* Corresponding author: Birger Marcusson (birger.marcusson@angstrom.uu.se).
The authors are with the Division for Electricity, Department of Engineering Sciences, Uppsala University, Box 534, SE-751 21 Uppsala, Sweden.

the stacking direction as long as the laminate end effects are considered. The anisotropic material can be defined to have effective permeabilities [2, 3] and equivalent, zero or near zero conductivity in the stacking direction [4–6]. The equivalent conductivity in the stacking direction goes to zero when the laminate sheet thickness divided by the laminate width goes to zero [4]. In this article, the derivation of Fourier series of magnetic and electric field components in the three-dimensional (3-D) case is done under the precondition that the conductivity in the stacking direction is much smaller than the conductivity in any direction perpendicular to the stacking direction.

Above a letter, $\bar{}$ denotes a complex quantity, $\tilde{}$ denotes a Fourier coefficient, and $\hat{}$ denotes an amplitude. Vectors and matrices are denoted by bold letters. Subscript c is used in the notation of Fourier coefficients that correspond to cosine eigenfunctions. The other Fourier coefficients correspond to sine eigenfunctions.

Section 2 contains fundamental assumptions and equations. In Section 2.1, Fourier series of fields in a laminate of width W and thickness T are derived. After a short derivation of the wave equation for the z component of the magnetic field strength, $\bar{\mathbf{H}}$, two-dimensional (2-D) Poisson equations for $\bar{H}_x$ and $\bar{H}_y$ are derived. The components of $\bar{\mathbf{H}}$ are the sums of two contributions, each corresponding to a subproblem of a boundary value problem. The boundary value problem for $\bar{H}_x$ is divided into two subproblems in three alternative ways that are compared. For $\bar{H}_y$, only one alternative is chosen. The choice of types of boundary conditions is motivated. Boundary conditions, eigenfunctions and propagation factors are determined. The Fourier series of $\bar{H}_z$ are given. The most complicated subproblems for $\bar{H}_x$ are solved. The solutions of the other subproblems are just subsets of the most complicated. Simple subproblems for $\bar{H}_y$ are solved. As a consequence of the 2-D Poisson equation, one of the two contributions of $\bar{H}_x$ and $\bar{H}_y$ is completely determined by $\bar{H}_z$. The Fourier series of the components of $\bar{\mathbf{E}}$ are expressed with Fourier coefficients of the components of $\bar{\mathbf{H}}$. Section 2.1.1 shows how the Fourier coefficients of Neumann boundary functions can be calculated. Section 2.2 contains shorted derivations of field expressions, amplitude relations, phase relations and eddy current density for traveling and standing waves along an infinite laminate with only one end surface. These cases could be of interest for both magnetic shielding and losses caused by magnetic leakage flux. Section 2.3 treats a slightly more general traveling wave case where the laminate thickness is arbitrary. In Section 3, FEA is compared to Fourier series in the 3-D case. Section 4 is mainly about sine interpolation and results of the 2-D cases.

2. DERIVATION OF HARMONICALLY TIME VARYING MAGNETIC AND ELECTRIC FIELD COMPONENTS

The z direction is the stacking direction, and the laminate is infinitely long in the x direction in all studied cases. Electromagnetic waves are assumed to sweep along the laminate in the x direction. In this direction the waves have the angular frequency, ω, the wave length, λ, and the wave propagation constant

$$k = \frac{2\pi}{\lambda}. \tag{1}$$

Maxwell's equations in complex form are

$$\nabla \cdot (\varepsilon \bar{\mathbf{E}}) = \rho, \tag{2}$$

$$\nabla \cdot \bar{\mathbf{B}} = 0, \tag{3}$$

$$\nabla \times \bar{\mathbf{E}} = -j\omega \bar{\mathbf{B}}, \tag{4}$$

$$\nabla \times \bar{\mathbf{H}} = \bar{\mathbf{J}} + j\omega\varepsilon \bar{\mathbf{E}} \tag{5}$$

where ε is the permittivity, ρ is the volume charge density, $\bar{\mathbf{B}}$ is the magnetic flux density, and $\bar{\mathbf{J}}$ is the current density. Anisotropic versions of relations of Ohm's law and between $\bar{\mathbf{B}}$ and $\bar{\mathbf{H}}$ are

$$\bar{\mathbf{J}} = \sigma_x \hat{\boldsymbol{x}} \bar{E}_x + \sigma_y \hat{\boldsymbol{y}} \bar{E}_y + \sigma_z \hat{\boldsymbol{z}} \bar{E}_z. \tag{6}$$

$$\bar{\mathbf{B}} = \mu_x \hat{\boldsymbol{x}} \bar{H}_x + \mu_y \hat{\boldsymbol{y}} \bar{H}_y + \mu_z \hat{\boldsymbol{z}} \bar{H}_z \tag{7}$$

where μ_i and σ_i for $i = x$, y or z are scalar, effective or assumed values of permeabilities and conductivities. The relations (6) and (7) are valid in the special case of diagonal conductivity and permeability tensors.

2.1. A Laminate with Width W and Thickness T in the Stacking Direction

Figure 1 shows a cross section of an anisotropic approximation of a laminate.

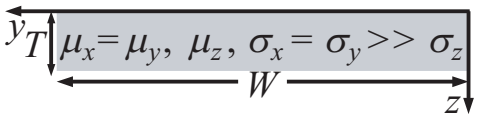

Figure 1. Cross section of an anisotropic approximation of a laminate of width W and thickness T. The relations $\mu_x = \mu_y$ and $\sigma_x = \sigma_y \gg \sigma_z$ are introduced in the derivation of equations whereas μ_z can be arbitrary.

Equations (5), (6) and (7) give that the z component of Eq. (4) can be written as

$$\hat{\boldsymbol{z}} \cdot \left(\nabla \times \bar{\mathbf{E}}\right) = -j\omega\mu_z \bar{H}_z = \frac{1}{\sigma_y + j\omega\varepsilon}\left(\frac{\partial^2 \bar{H}_x}{\partial x \partial z} - \frac{\partial^2 \bar{H}_z}{\partial x^2}\right) - \frac{1}{\sigma_x + j\omega\varepsilon}\left(\frac{\partial^2 \bar{H}_z}{\partial y^2} - \frac{\partial^2 \bar{H}_y}{\partial y \partial z}\right) \tag{8}$$

In the special case where $\mu_x = \mu_y$ and $\sigma_x = \sigma_y$, Eqs. (3) and (8) give the wave equation

$$Q\left(\frac{\partial^2 \bar{H}_z}{\partial x^2} + \frac{\partial^2 \bar{H}_z}{\partial y^2}\right) + \frac{\partial^2 \bar{H}_z}{\partial z^2} = \bar{\gamma}^2 \bar{H}_z \tag{9}$$

where $Q = \mu_x/\mu_z$, and

$$\bar{\gamma}^2 = -\omega^2 \mu_x \varepsilon + j\omega\mu_x\sigma_y. \tag{10}$$

Uncoupled wave equations for $\bar{H}_x$ and $\bar{H}_y$ can not be obtained as easily as for $\bar{H}_z$ because of the anisotropy. A way to get approximative values of $\bar{H}_x$ and $\bar{H}_y$ is to use the solution of Eq. (9) as a source term in simplified equations for $\bar{H}_x$ and $\bar{H}_y$. These simplified equations are derived next. Eqs. (5), (6) and (7) give that the x component of Eq. (4) multiplied by $\sigma_z + j\omega\varepsilon$ can be written as

$$\hat{\boldsymbol{x}} \cdot (\nabla \times \bar{\mathbf{E}})(\sigma_z + j\omega\varepsilon) = -j\omega\mu_x(\sigma_z + j\omega\varepsilon)\bar{H}_x = \left(\frac{\partial^2 \bar{H}_y}{\partial x \partial y} - \frac{\partial^2 \bar{H}_x}{\partial y^2}\right) - \frac{\sigma_z + j\omega\varepsilon}{\sigma_y + j\omega\varepsilon}\left(\frac{\partial^2 \bar{H}_x}{\partial z^2} - \frac{\partial^2 \bar{H}_z}{\partial x \partial z}\right) \tag{11}$$

Under the conditions that $\sigma_y \gg \sigma_z$, $\sigma_y \gg \omega\varepsilon$, and that all terms in Eq. (11) that contain the factor $\sigma_z + j\omega\varepsilon$ can be neglected, Eq. (11) can be approximated by

$$\frac{\partial^2 \bar{H}_y}{\partial x \partial y} = \frac{\partial^2 \bar{H}_x}{\partial y^2}. \tag{12}$$

With use of Eqs. (3), (7) and $\mu_x = \mu_y$, the derivative $\frac{\partial \bar{H}_y}{\partial y}$ on the left hand side of Eq. (12) can be replaced, and Eq. (12) can be written as

$$\frac{\partial^2 \bar{H}_x}{\partial x^2} + \frac{\partial^2 \bar{H}_x}{\partial y^2} = -\frac{1}{Q}\frac{\partial^2 \bar{H}_z}{\partial x \partial z} \tag{13}$$

which is a 2-D Poisson equation for $\bar{H}_x$ with $\bar{H}_z$ known from the solution of Eq. (9). The Poisson equation can be considered to be 2-D since there is no differentiation with respect to z on the left hand side. Similarly,

$$\frac{\partial^2 \bar{H}_y}{\partial x^2} + \frac{\partial^2 \bar{H}_y}{\partial y^2} = -\frac{1}{Q}\frac{\partial^2 \bar{H}_z}{\partial y \partial z}. \tag{14}$$

The geometry in Fig. 1 is such that there can be two pairs of boundaries with non-periodic inhomogeneous boundary conditions. In this case, each field component, H_i, with $i = x$, y or z, can be written as a sum of two contributions, H_{i1} and H_{i2}, that each satisfies the conditions for use of Fourier's method, as in the case with isotropic plates [7]. Following the separation of each field component into two contributions is the separation of each of Eqs. (13) and (14) into two equations such that their sum is equal to Eq. (13) or (14). (Three contributions and equations per field component can be used if the

source term is treated in a separate problem [8].) Equations from three alternative divisions of Eq. (13) are

$$\nabla_{xy}^2 \bar{H}_{x1} = -\frac{1}{Q}\frac{\partial^2 \bar{H}_{z1}}{\partial x \partial z} \qquad \nabla_{xy}^2 \bar{H}_{x2} = -\frac{1}{Q}\frac{\partial^2 \bar{H}_{z2}}{\partial x \partial z} \tag{15}$$

$$\nabla_{xy}^2 \bar{H}_{x1} = -\frac{1}{Q}\frac{\partial^2 \bar{H}_{z}}{\partial x \partial z} \qquad \nabla_{xy}^2 \bar{H}_{x2} = 0 \tag{16}$$

$$\nabla_{xy}^2 \bar{H}_{x1} = 0 \qquad \nabla_{xy}^2 \bar{H}_{x2} = -\frac{1}{Q}\frac{\partial^2 \bar{H}_{z}}{\partial x \partial z} \tag{17}$$

where $\nabla_{xy}^2 = \partial^2/\partial x^2 + \partial^2/\partial y^2$. The orthogonality of eigenfunctions can be used to simplify determination of Fourier coefficients of $\bar{H}_{x1}$ and $\bar{H}_{x2}$ if at least partly the same eigenfunctions are used on the left hand sides as on the right hand sides of Eqs. (15)–(17). Eq. (15) offers the most advantage of the orthogonality. Eqs. (16) and (17) give integral expressions that are relatively time consuming to calculate. If $\bar{H}_{x1}$ is chosen to have y dependent eigenfunctions, alternative (17) has the advantage of giving $\bar{H}_{x1} = 0$. Eq. (14) can be divided in the same way as Eq. (13) but only

$$\nabla_{xy}^2 \bar{H}_{y1} = -\frac{1}{Q}\frac{\partial^2 \bar{H}_{z1}}{\partial y \partial z} \qquad \nabla_{xy}^2 \bar{H}_{y2} = -\frac{1}{Q}\frac{\partial^2 \bar{H}_{z2}}{\partial y \partial z} \tag{18}$$

is used in this article. For each of the equations in Eqs. (15) and (18), there are two possible combinations of Dirichlet and Neumann conditions that allow mode-wise identification between the left hand side and the right hand side. That gives a total of four possible combinations for $\bar{\mathbf{H}}$ since the choices for $\bar{H}_{i1}$ and $\bar{H}_{i2}$ are independent, $i = x$, y or z. For each $\bar{\mathbf{H}}$ component, one choice, here called *Choice 1*, is to use Neumann conditions on every boundary surface to which the $\bar{\mathbf{H}}$ component is tangential and Dirichlet conditions on the other boundary surfaces. This choice turns out to give excellent $\bar{\mathbf{H}}$ field agreement between Fourier series and FEA but makes $\bar{E}_x$ and $\bar{E}_y$ discontinuous at $z = 0$ and T because of z dependent sine eigenfunctions. This defect can be fixed by replacement of the $\bar{E}_x$ and $\bar{E}_y$ values at $z = 0$ and T by extrapolated values. Since there is no differentiation of $\bar{H}_x$ and $\bar{H}_y$ with respect to z in Eqs. (13) and (14), inhomogeneous boundary conditions on $\bar{H}_x$ and $\bar{H}_y$ at constant z can be used only indirectly or not at all in order not to overdetermine $\bar{H}_x$ and $\bar{H}_y$. Indirect use in this case means that boundary conditions on $\bar{H}_x$ and $\bar{H}_y$ are used in the calculation of the inhomogeneous boundary conditions on $\bar{H}_z$. Advantages of *Choice 1* are that inhomogeneous boundary conditions on $\bar{H}_x$ and $\bar{H}_y$ at constant z are not needed, and no $\bar{\mathbf{H}}$ component is forced to zero by sine eigenfunctions on any edge. However, in order to give $\bar{E}_x$ and $\bar{E}_y$ z dependent cosine eigenfunctions, another choice of boundary conditions will be used below. This choice gives better $\bar{\mathbf{E}}$ field agreement between Fourier series and FEA but extrapolation of the $\bar{\nu}$ dependent part of $\bar{E}_y$ may still be required unless boundary field values are very accurate. The $\bar{\mathbf{H}}$ components satisfy the periodic boundary conditions

$$\bar{H}_i(x,y,z) = \bar{H}_i(x+\lambda,y,z) \qquad \frac{\partial \bar{H}_i(x,y,z)}{\partial x} = \frac{\partial \bar{H}_i(x+\lambda,y,z)}{\partial x}, \quad i = x, y \text{ or } z. \tag{19}$$

The non-periodic boundary conditions are

$$\frac{\partial \bar{H}_{x1}}{\partial y}(x,0,z) = 0 \qquad \frac{\partial \bar{H}_{x1}}{\partial y}(x,W,z) = 0 \tag{20}$$

$$\frac{\partial \bar{H}_{x2}}{\partial y}(x,0,z) = \bar{F}_x^{y=0}(z)e^{-jkx} \qquad \frac{\partial \bar{H}_{x2}}{\partial y}(x,W,z) = \bar{F}_x^{y=W}(z)e^{-jkx} \tag{21}$$

$$\bar{H}_{x1}(x,y,0) = \bar{f}_x^{z=0}(y)e^{-jkx} \qquad \bar{H}_{x1}(x,y,T) = \bar{f}_x^{z=T}(y)e^{-jkx} \tag{22}$$

$$\bar{H}_{x2}(x,y,0) = 0 \qquad \bar{H}_{x2}(x,y,T) = 0 \tag{23}$$

$$\bar{H}_{y1}(x,0,z) = 0 \qquad \bar{H}_{y1}(x,W,z) = 0 \tag{24}$$

$$\bar{H}_{y2}(x,0,z) = \bar{f}_y^{y=0}(z)e^{-jkx} \qquad \bar{H}_{y2}(x,W,z) = \bar{f}_y^{y=W}(z)e^{-jkx} \tag{25}$$

$$\bar{H}_{y1}(x,y,0) = \bar{f}_y^{z=0}(y)e^{-jkx} \qquad \bar{H}_{y1}(x,y,T) = \bar{f}_y^{z=T}(y)e^{-jkx} \tag{26}$$

$$\bar{H}_{y2}(x,y,0)=0 \qquad \bar{H}_{y2}(x,y,T)=0 \tag{27}$$

$$\frac{\partial \bar{H}_{z1}}{\partial y}(x,0,z)=0 \qquad \frac{\partial \bar{H}_{z1}}{\partial y}(x,W,z)=0 \tag{28}$$

$$\frac{\partial \bar{H}_{z2}}{\partial y}(x,0,z)=\bar{F}_z^{y=0}(z)e^{-jkx} \qquad \frac{\partial \bar{H}_{z2}}{\partial y}(x,W,z)=\bar{F}_z^{y=W}(z)e^{-jkx} \tag{29}$$

$$\frac{\partial \bar{H}_{z1}}{\partial y}(x,y,0)=\bar{F}_z^{z=0}(y)e^{-jkx} \qquad \frac{\partial \bar{H}_{z1}}{\partial y}(x,y,T)=\bar{F}_z^{z=T}(y)e^{-jkx} \tag{30}$$

$$\frac{\partial \bar{H}_{z2}}{\partial y}(x,y,0)=0 \qquad \frac{\partial \bar{H}_{z2}}{\partial y}(x,y,T)=0 \tag{31}$$

where $\bar{f}$ and $\bar{F}$ are boundary functions. A Fourier series of $\bar{H}_{z1}$ with terms of the form $\bar{X}_m(x)\bar{Y}_n(y)\bar{\bar{Z}}_{m,n}(z)$ inserted in Eq. (9) gives

$$Q\frac{\bar{X}_m''}{\bar{X}_m}+Q\frac{\bar{Y}_n''}{\bar{Y}_n}+\frac{\bar{\bar{Z}}_{m,n}''}{\bar{\bar{Z}}_{m,n}}=\bar{\gamma}^2 \tag{32}$$

where all terms on the left side must be constants since they are independent and have a constant sum. Eq. (32) can therefore be separated into the three equations

$$\bar{X}_m''(x)+\vartheta_m^2\bar{X}_m(x)=0 \qquad \bar{Y}_n''(y)+K_n^2\bar{Y}_n(y)=0 \qquad \bar{\bar{Z}}_{m,n}''(z)=\bar{\eta}_{m,n}^2\bar{\bar{Z}}_{m,n}(z). \tag{33}$$

where $\vartheta_m=mk$ and $K_n=n\pi/W$ are eigenvalues. The general solution of the last equation in Eq. (33) is

$$\bar{\bar{Z}}_{m,n}=\bar{C}_{m,n}e^{\bar{\eta}z}+\bar{D}_{m,n}e^{-\bar{\eta}z}. \tag{34}$$

The equations in Eq. (33) inserted in Eq. (32) give

$$\bar{\eta}_{m,n}^2=\bar{\gamma}^2+Q\left(\vartheta_m^2+K_n^2\right) \qquad a_{m,n}=Q\left(\vartheta_m^2+K_n^2\right)-\omega^2\mu_x\varepsilon \qquad b=\omega\mu_x\sigma_y \tag{35}$$

where $a_{m,n}$ is the real part and b is the imaginary part of $\bar{\eta}_{m,n}^2$. A Fourier series of $\bar{H}_{z2}$ with terms of the form $\bar{X}_m(x)\bar{\bar{Y}}_{l,m}(y)\bar{Z}_l(z)$ inserted in Eq. (9) gives

$$Q\frac{\bar{X}_m''}{\bar{X}_m}+Q\frac{\bar{\bar{Y}}_{l,m}''}{\bar{\bar{Y}}_{l,m}}+\frac{\bar{Z}_l''}{\bar{Z}_l}=\bar{\gamma}^2 \tag{36}$$

which can be separated into the three equations

$$\bar{X}_m''(x)+\vartheta_m^2\bar{X}_m(x)=0 \qquad \bar{Z}_l''(z)+\kappa_l^2\bar{Z}_l(z)=0 \qquad \bar{\bar{Y}}_{l,m}''(y)=\bar{\nu}_{l,m}^2\bar{\bar{Y}}_{l,m}(y) \tag{37}$$

where $\kappa_l=l\pi/T$ is an eigenvalue. The equations in Eq. (37) inserted in Eq. (36) give

$$\bar{\nu}_{l,m}^2=\frac{\bar{\gamma}^2+\kappa_l^2}{Q}+\vartheta_m^2 \qquad c_{l,m}=\vartheta_m^2+\frac{1}{Q}\left(\kappa_l^2-\omega^2\mu_x\varepsilon\right) \qquad d=\frac{\omega\mu_x\sigma_y}{Q} \tag{38}$$

where $c_{l,m}$ is the real part and d is the imaginary part of $\bar{\nu}_{l,m}^2$. The mathematical expressions for the eigenfunctions $\bar{X}_m$, $\bar{Y}_n$ and $\bar{Z}_l$ expressed as functions of ϑ_m, K_n, κ_l and coordinates are the same as for plates with isotropic materials [7]. Also the expressions for the real and imaginary parts of $\bar{\eta}_{m,n}$ in terms of $a_{m,n}$ and b, and of $\bar{\nu}_{l,m}$ in terms of $c_{l,m}$ and d, are the same as in the isotropic cases. The form of a Fourier coefficient expressed with hyperbolic functions depends on the types of the inhomogeneous boundary conditions on one subset of boundaries whereas the eigenfunctions depend on the types of the homogeneous boundary conditions on the other boundaries. The solutions of Eq. (9) with Eqs. (19) and (28)–(31) are

$$\bar{H}_{z1}(x,y,z)=e^{-jkx}\sum_{n=0}^{\infty}\left(\bar{\bar{F}}_{z,\mathrm{c},n}^{z=T}\cosh\bar{\eta}_n z-\bar{\bar{F}}_{z,\mathrm{c},n}^{z=0}\cosh\bar{\eta}_n(T-z)\right)\frac{\cos K_n y}{\bar{\eta}_n\sinh\bar{\eta}_n T}, \tag{39}$$

$$\bar{H}_{z2}(x,y,z)=e^{-jkx}\sum_{l=0}^{\infty}\left(\bar{\bar{F}}_{z,\mathrm{c},l}^{y=W}\cosh\bar{\nu}_l y-\bar{\bar{F}}_{z,\mathrm{c},l}^{y=0}\cosh\bar{\nu}_l(W-y)\right)\frac{\cos\kappa_l z}{\bar{\nu}_l\sinh\bar{\nu}_l W}. \tag{40}$$

A Fourier series of $\bar{H}_{x1}$ that satisfies Eq. (20) and can give term-wise equality in the first equation in Eq. (15) is

$$\bar{H}_{x1}(x,y,z) = e^{-jkx}\sum_{n=0}^{\infty}\bar{\bar{H}}_{x1,\mathrm{c},n}(z)\cos K_n y \tag{41}$$

Equations. (39)–(41) inserted in the equation for $\bar{H}_{x1}$ in Eq. (16) give

$$\begin{aligned}\sum_{n=0}^{\infty}\bar{\bar{H}}_{x1,\mathrm{c},n}(z)(-k^2-K_n^2)\cos K_n y \;=\; & \frac{jk}{Q}\sum_{n=0}^{\infty}\left(\bar{\bar{F}}^{z=T}_{z,\mathrm{c},n}\sinh\bar{\eta}_n z+\bar{\bar{F}}^{z=0}_{z,\mathrm{c},n}\sinh\bar{\eta}_n(T-z)\right)\frac{\cos K_n y}{\sinh\bar{\eta}_n T}\\ & +\frac{jk}{Q}\sum_{l=1}^{\infty}\left(\bar{\bar{F}}^{y=0}_{z,\mathrm{c},l}\cosh\bar{\nu}_l(W-y)-\bar{\bar{F}}^{y=W}_{z,\mathrm{c},l}\cosh\bar{\nu}_l y\right)\frac{\kappa_l\sin\kappa_l z}{\bar{\nu}_l\sinh\bar{\nu}_l W}.\end{aligned} \tag{42}$$

It can be noted that the left hand side of Eq. (42) is written as a Fourier series because of the particular combination of coordinate dependence and 2-D Poisson equation. The orthogonality can now be used to extract a single term, e.g., for mode $n = n_0$ in the series in Eq. (42). Multiplication of Eq. (42) by $\cos K_{n_0} y$ followed by integration from $y = 0$ to W gives

$$\bar{\bar{H}}_{x1,\mathrm{c},n}(z)=\frac{-jk}{(k^2+K_n^2)Q\sinh\bar{\eta}_n T}\left(\bar{\bar{F}}^{z=T}_{z,\mathrm{c},n}\sinh\bar{\eta}_n z+\bar{\bar{F}}^{z=0}_{z,\mathrm{c},n}\sinh\bar{\eta}_n(T-z)\right)-\frac{2\bar{I}_{xz2}(z)}{(k^2+K_n^2)(1+\delta_{n,0})W} \tag{43}$$

where mode index n is used instead of n_0 for compactness, $\delta_{n,0} = 1$ if $n = 0$, $\delta_{n,0} = 0$ if $n \neq 0$, and

$$\bar{I}_{xz2,n}(z) = \frac{jk}{Q}\int_0^W\sum_{l=1}^{\infty}\left(\bar{\bar{F}}^{y=0}_{z,\mathrm{c},l}\cosh\bar{\nu}_l(W-y)-\bar{\bar{F}}^{y=W}_{z,\mathrm{c},l}\cosh\bar{\nu}_l y\right)\frac{\kappa_l\sin\kappa_l z}{\bar{\nu}_l\sinh\bar{\nu}_l W}\cos K_n y\,\mathrm{d}y. \tag{44}$$

It is clear from Eq. (43) that the source term alone determines $\bar{\bar{H}}_{x1,\mathrm{c},n}$ completely, without explicit use of inhomogeneous boundary conditions on $\bar{H}_{x1,n}$. However, $\bar{\bar{F}}^{z=T}_{z,\mathrm{c},n}$ and $\bar{\bar{F}}^{z=0}_{z,\mathrm{c},n}$ depend on the inhomogeneous boundary conditions on $\bar{H}_{x1,n}$ and $\bar{H}_{y1,n}$. This is shown in Section 2.1.1. In case of Eq. (15), $\bar{\bar{H}}_{x1,\mathrm{c},n}$ is given by Eq. (43) without $\bar{I}_{xz2,n}$. In case of Eq. (17), the right hand side of Eq. (42) is zero which, with use of the orthogonality, gives $\bar{\bar{H}}_{x1,\mathrm{c},n} = 0$. A Fourier series of $\bar{H}_{x2}$ that satisfies Eq. (23) and can give term-wise equality in the second equation in Eq. (15) is

$$\bar{H}_{x2}(x,y,z) = e^{-jkx}\sum_{l=1}^{\infty}\bar{\bar{H}}_{x2,l}(y)\sin\kappa_l z \tag{45}$$

Equations (39), (40) and (45) inserted in the equation for $\bar{H}_{x2}$ in Eq. (17) give

$$\begin{aligned}\sum_{l=1}^{\infty}\left(-k^2\bar{\bar{H}}_{x2,l}(y)+\bar{\bar{H}}''_{x2,l}(y)\right)\sin\kappa_l z \;=\; & \frac{jk}{Q}\sum_{n=0}^{\infty}\left(\bar{\bar{F}}^{z=T}_{z,\mathrm{c},n}\sinh\bar{\eta}_n z+\bar{\bar{F}}^{z=0}_{z,\mathrm{c},n}\sinh\bar{\eta}_n(T-z)\right)\frac{\cos K_n y}{\sinh\bar{\eta}_n T}\\ & +\frac{jk}{Q}\sum_{l=1}^{\infty}\left(\bar{\bar{F}}^{y=0}_{z,\mathrm{c},l}\cosh\bar{\nu}_l(W-y)-\bar{\bar{F}}^{y=W}_{z,\mathrm{c},l}\cosh\bar{\nu}_l y\right)\frac{\kappa_l\sin\kappa_l z}{\bar{\nu}_l\sinh\bar{\nu}_l W}.\end{aligned} \tag{46}$$

Multiplication of Eq. (46) by $\sin\kappa_{l_0} z$ followed by integration from $z = 0$ to T gives

$$-k^2\bar{\bar{H}}_{x2,l}(y)+\bar{\bar{H}}''_{x2,l}(y) = jk\bar{G}_l(y)+\frac{2\bar{I}_{xz1,l}(y)}{T} \tag{47}$$

where mode index l is used instead of l_0 for compactness, and

$$\bar{G}_l(y) \;=\; \kappa_l\frac{\bar{\bar{F}}^{y=0}_{z,\mathrm{c},l}\cosh\bar{\nu}_l(W-y)-\bar{\bar{F}}^{y=W}_{z,\mathrm{c},l}\cosh\bar{\nu}_l y}{Q\bar{\nu}_l\sinh\bar{\nu}_l W} \tag{48}$$

$$\begin{aligned}\bar{I}_{xz1,l}(y) \;&=\; \frac{jk}{Q}\int_0^T\sum_{n=0}^{\infty}\left(\bar{\bar{F}}^{z=T}_{z,\mathrm{c},n}\sinh\bar{\eta}_n z+\bar{\bar{F}}^{z=0}_{z,\mathrm{c},n}\sinh\bar{\eta}_n(T-z)\right)\frac{\cos K_n y}{\sinh\bar{\eta}_n T}\sin\kappa_l z\,\mathrm{d}z\\ &=\; \sum_{n=0}^{\infty}\bar{I}_{xz1,l,n}\cos K_n y.\end{aligned} \tag{49}$$

A particular solution of Eq. (47) can be written as a sum. Each term in the sum corresponds to one of the terms in Eq. (48) or (49). The general solution of Eq. (47) is

$$\bar{\tilde{H}}_{x2,l}(y) = \bar{C}_{x,l}e^{ky} + \bar{D}_{x,l}e^{-ky} + \frac{jk\bar{G}_l(y)}{\bar{\nu}_l^2 - k^2} - \frac{2}{T}\sum_{n=0}^{\infty}\frac{\bar{I}_{xz1,l,n}}{k^2 + K_n^2}\cos K_n y \tag{50}$$

where the two first terms satisfy the homogeneous equation obtained from Eq. (47) by replacement of the right hand side by 0, and $\bar{C}_{x,l}$ and $\bar{D}_{x,l}$ are determined below. Fourier series of Eq. (21) with the eigenfunctions of Eq. (45) are

$$\frac{\partial \bar{H}_{x2}}{\partial y}(x,0,z) = e^{-jkx}\sum_{l=1}^{\infty}\bar{\tilde{F}}_{x,l}^{y=0}\sin\kappa_l z \qquad \frac{\partial \bar{H}_{x2}}{\partial y}(x,W,z) = e^{-jkx}\sum_{l=1}^{\infty}\bar{\tilde{F}}_{x,l}^{y=W}\sin\kappa_l z. \tag{51}$$

Equations (48), (45), (50) and (51) give

$$\bar{C}_{x,l} = \frac{\bar{\Delta}_{xz,l}^{y=W} - \bar{\Delta}_{xz,l}^{y=0}e^{-kW}}{2\sinh kW} \qquad \bar{D}_{x,l} = \frac{\bar{\Delta}_{xz,l}^{y=W} - \bar{\Delta}_{xz,l}^{y=0}e^{kW}}{2\sinh kW} \tag{52}$$

where

$$\bar{\Delta}_{xz,l}^{y=0} = \frac{\bar{\tilde{F}}_{x,l}^{y=0}}{k} - \frac{j\kappa_l\bar{\tilde{F}}_{z,\mathrm{c},l}^{y=0}}{(k^2 - \bar{\nu}_l^2)Q} \qquad \bar{\Delta}_{xz,l}^{y=W} = \frac{\bar{\tilde{F}}_{x,l}^{y=W}}{k} - \frac{j\kappa_l\bar{\tilde{F}}_{z,\mathrm{c},l}^{y=W}}{(k^2 - \bar{\nu}_l^2)Q}. \tag{53}$$

In case of Eq. (15), $\bar{\tilde{H}}_{x2,l}$ is given by Eq. (50) without $\bar{I}_{xz1,l,n}$. In case of Eq. (16), $\bar{\tilde{H}}_{x2,l}$ is given by Eq. (50) without $\bar{G}_l$ and $\bar{I}_{xz1,l,n}$. In the absence of $\bar{G}_l$, terms with $\bar{\tilde{F}}_{z,l}$ are absent from Eq. (53).

A Fourier series of $\bar{H}_{y1}$ that satisfies Eq. (24) and can give term-wise equality in the first equation in Eq. (18) is

$$\bar{H}_{y1}(x,y,z) = e^{-jkx}\sum_{n=1}^{\infty}\bar{\tilde{H}}_{y1,n}(z)\sin K_n y \tag{54}$$

Equations (39) and (54) inserted in the first equation in Eq. (18) give

$$\sum_{n=1}^{\infty}\bar{\tilde{H}}_{y1,n}(z)\left(-k^2 - K_n^2\right)\sin K_n y = \frac{1}{Q}\sum_{n=1}^{\infty}\left(\bar{\tilde{F}}_{z,\mathrm{c},n}^{z=T}\sinh\bar{\eta}_n z + \bar{\tilde{F}}_{z,\mathrm{c},n}^{z=0}\sinh\bar{\eta}_n(T-z)\right)\frac{K_n\sin K_n y}{\sinh\bar{\eta}_n T} \tag{55}$$

Multiplication of Eq. (55) by $\sin K_{n_0}y$ followed by integration from $y = 0$ to W gives, after replacement of symbol n_0 by n,

$$\bar{\tilde{H}}_{y1,n}(z) = -\frac{K_n\left(\bar{\tilde{F}}_{z,\mathrm{c},n}^{z=T}\sinh\bar{\eta}_n z + \bar{\tilde{F}}_{z,\mathrm{c},n}^{z=0}\sinh\bar{\eta}_n(T-z)\right)}{(k^2 + K_n^2)Q\sinh\bar{\eta}_n T} \tag{56}$$

A Fourier series of $\bar{H}_{y2}$ that satisfies Eq. (27) and can give term-wise equality in the second equation in Eq. (18) is

$$\bar{H}_{y2}(x,y,z) = e^{-jkx}\sum_{l=1}^{\infty}\bar{\tilde{H}}_{y2,l}(y)\sin\kappa_l z \tag{57}$$

Equations (40) and (57) inserted in the second equation in Eq. (18) give

$$\sum_{l=0}^{\infty}\left(-k^2\bar{\tilde{H}}_{y2,l}(y) + \bar{\tilde{H}}''_{y2,l}(y)\right)\sin\kappa_l z = \frac{1}{Q}\sum_{l=1}^{\infty}\left(\bar{\tilde{F}}_{z,\mathrm{c},l}^{y=W}\sinh\bar{\nu}_l y + \bar{\tilde{F}}_{z,\mathrm{c},l}^{y=0}\sinh\bar{\nu}_l(W-y)\right)\frac{\kappa_l\sin\kappa_l z}{\sinh\bar{\nu}_l W}. \tag{58}$$

Multiplication of Eq. (58) by $\sin\kappa_{l_0}z$ followed by integration from $z = 0$ to T gives, after replacement of symbol l_0 by l,

$$k^2\bar{\tilde{H}}_{y2,l}(y) - \bar{\tilde{H}}''_{y2,l}(y) = \bar{G}'_l(y) \tag{59}$$

The general solution to Eq. (59) is

$$\bar{\tilde{H}}_{y2,l}(y) = \bar{C}_{y,l}e^{ky} + \bar{D}_{y,l}e^{-ky} + \frac{\bar{G}'_l(y)}{k^2 - \bar{\nu}_l^2} \tag{60}$$

where the last term is a particular solution, and $\bar{C}_{y,l}$ and $\bar{D}_{y,l}$ are determined below. Fourier series of Eq. (25) with the eigenfunctions of Eq. (57) are

$$\bar{H}_{y2}(x,0,z) = e^{-jkx}\sum_{l=1}^{\infty}\bar{\bar{f}}_{y,l}^{y=0}\sin\kappa_l z \qquad \bar{H}_{y2}(x,W,z) = e^{-jkx}\sum_{l=1}^{\infty}\bar{\bar{f}}_{y,l}^{y=W}\sin\kappa_l z. \tag{61}$$

Equations (48), (57), (60) and (61) give

$$\bar{C}_{y,l} = \frac{\bar{\Delta}_{yz,l}^{y=W} - \bar{\Delta}_{yz,l}^{y=0}e^{-kW}}{2\sinh kW} \qquad \bar{D}_{y,l} = \frac{\bar{\Delta}_{yz,l}^{y=0}e^{kW} - \bar{\Delta}_{yz,l}^{y=W}}{2\sinh kW} \tag{62}$$

where

$$\bar{\Delta}_{yz,l}^{y=0} = \bar{\bar{f}}_{y,l}^{y=0} - \frac{\kappa_l\bar{\bar{F}}_{z,\mathrm{c},l}^{y=0}}{(\bar{\nu}_l^2-k^2)Q} \qquad \bar{\Delta}_{yz,l}^{y=W} = \bar{\bar{f}}_{y,l}^{y=W} - \frac{\kappa_l\bar{\bar{F}}_{z,\mathrm{c},l}^{y=W}}{(\bar{\nu}_l^2-k^2)Q}. \tag{63}$$

Equations (5), (39), (40), (41), (43), (45), (50), (54), (56), (57) and (60) give that the $\bar{\mathbf{E}}$ field contributions can be written as

$$\bar{E}_{x\eta}(x,y,z) = \frac{e^{-jkx}}{\sigma_x+j\omega\varepsilon}\sum_{n=1}^{\infty}\left(\bar{\bar{F}}_{z,\mathrm{c},n}^{z=0}\cosh\bar{\eta}_n(T-z) - \bar{\bar{F}}_{z,\mathrm{c},n}^{z=T}\cosh\bar{\eta}_n z\right)\left(1-\frac{\bar{\eta}_n^2}{(k^2+K_n^2)Q}\right)\frac{K_n\sin K_n y}{\bar{\eta}_n\sinh\bar{\eta}_n T} \tag{64}$$

$$\begin{aligned}\bar{E}_{x\nu}(x,y,z) = \frac{e^{-jkx}}{\sigma_x+j\omega\varepsilon}\Bigg\{&\frac{\bar{\bar{F}}_{z,\mathrm{c},0}^{y=W}\sinh\bar{\nu}_0 y + \bar{\bar{F}}_{z,\mathrm{c},0}^{y=0}\sinh\bar{\nu}_0(W-y)}{\sinh\bar{\nu}_0 W}\\ &-\sum_{l=1}^{\infty}\left[\left(\bar{C}_{y,l}e^{ky}+\bar{D}_{y,l}e^{-ky}\right)\kappa_l + \left(\frac{\kappa_l}{k^2-\bar{\nu}_l^2}+\frac{Q}{\kappa_l}\right)\bar{G}_l'(y)\right]\cos\kappa_l z\Bigg\}\end{aligned} \tag{65}$$

$$\bar{E}_{y\eta}(x,y,z) = \frac{jke^{-jkx}}{\sigma_y+j\omega\varepsilon}\sum_{n=0}^{\infty}\left(\bar{\bar{F}}_{z,\mathrm{c},n}^{z=0}\cosh\bar{\eta}_n(T-z) - \bar{\bar{F}}_{z,\mathrm{c},n}^{z=T}\cosh\bar{\eta}_n z\right)\left(\frac{\bar{\eta}_n^2}{(k^2+K_n^2)Q}-1\right)\frac{\cos K_n y}{\bar{\eta}_n\sinh\bar{\eta}_n T} \tag{66}$$

$$\begin{aligned}\bar{E}_{y\nu}(x,y,z) = \frac{jke^{-jkx}}{\sigma_y+j\omega\varepsilon}\Bigg\{&\frac{\bar{\bar{F}}_{z,\mathrm{c},0}^{y=W}\cosh\bar{\nu}_0 y - \bar{\bar{F}}_{z,\mathrm{c},0}^{y=0}\cosh\bar{\nu}_0(W-y)}{\bar{\nu}_0\sinh\bar{\nu}_0 W}\\ &+\sum_{l=1}^{\infty}\left[\left(\bar{C}_{x,l}e^{ky}+\bar{D}_{x,l}e^{-ky}\right)\kappa_l + \left(\frac{\kappa_l}{\bar{\nu}_l^2-k^2}-\frac{Q}{\kappa_l}\right)jk\bar{G}_l(y)\right]\cos\kappa_l z\Bigg\}\end{aligned} \tag{67}$$

$$\bar{E}_z(x,y,z) = \frac{ke^{-jkx}}{\sigma_z+j\omega\varepsilon}\sum_{l=0}^{\infty}\left(\left(\bar{D}_{x,l}-j\bar{D}_{y,l}\right)e^{-ky} - \left(\bar{C}_{x,l}+j\bar{C}_{y,l}\right)e^{ky}\right)\sin\kappa_l z \tag{68}$$

where $\bar{E}_{x\eta}+\bar{E}_{x\nu}=\bar{E}_x$ and $\bar{E}_{y\eta}+\bar{E}_{y\nu}=\bar{E}_y$. The average eddy current loss density during a cycle is

$$p = \frac{1}{2}\bar{\mathbf{J}}\cdot\bar{\mathbf{E}}^* = \frac{1}{2}\left(\sigma_x\widehat{E}_x^2+\sigma_y\widehat{E}_y^2+\sigma_z\widehat{E}_z^2\right). \tag{69}$$

2.1.1. Determination of Neumann Boundary Functions

Ampère's law and tangential $\bar{\mathbf{E}}$ components can be used for determination of normal derivatives of tangential $\bar{\mathbf{H}}$ components, such as $\bar{H}_{x2}$ and $\bar{H}_{z2}$ at $y=0$ and W, as described in [7]. The normal derivative of a normal $\bar{\mathbf{H}}$ component, such as $\bar{H}_{z1}$ at $z=0$ and T, can be calculated from Eqs. (3), (7) and the boundary values of the tangential $\bar{\mathbf{H}}$ components. Fourier series of $\bar{E}_{x2}(x,0,z)$, $\bar{E}_{x2}(x,W,z)$, $\bar{E}_{z2}(x,0,z)$, and $\bar{E}_{z2}(x,W,z)$ with eigenfunctions that can give term-wise identification of Fourier coefficients in Ampère's law are

$$\bar{E}_{x2}(x,0,z) = e^{-jkx}\sum_{l=0}^{\infty}\bar{\bar{g}}_{x,\mathrm{c},l}^{y=0}\cos\kappa_l z \qquad \bar{E}_{x2}(x,W,z) = e^{-jkx}\sum_{l=0}^{\infty}\bar{\bar{g}}_{x,\mathrm{c},l}^{y=W}\cos\kappa_l z \tag{70}$$

$$\bar{E}_{z2}(x,0,z) = e^{-jkx}\sum_{l=1}^{\infty}\bar{\bar{g}}_{z,l}^{y=0}\sin\kappa_l z \qquad \bar{E}_{z2}(x,W,z) = e^{-jkx}\sum_{l=1}^{\infty}\bar{\bar{g}}_{z,l}^{y=W}\sin\kappa_l z \tag{71}$$

Equations (5), (40), (51), (61), (70) and the orthogonality of the eigenfunctions give

$$\bar{\tilde{F}}^{y=0}_{sz,c,l} = \kappa_{s,l}\frac{\mu_{a,y}}{\mu_{s,y}}\bar{\tilde{f}}^{y=0}_{ay,l} + (\sigma_{s,x} + j\omega\varepsilon_s)\bar{\tilde{g}}^{y=0}_{x,c,l} \qquad \bar{\tilde{F}}^{y=W}_{sz,c,l} = \kappa_{s,l}\frac{\mu_{a,y}}{\mu_{s,y}}\bar{\tilde{f}}^{y=W}_{ay,l} + (\sigma_{s,x} + j\omega\varepsilon_s)\bar{\tilde{g}}^{y=W}_{x,c,l} \tag{72}$$

$$\bar{\tilde{F}}^{y=0}_{sx,l} = -jk\frac{\mu_{a,y}}{\mu_{s,y}}\bar{\tilde{f}}^{y=0}_{ay,l} - (\sigma_{s,z} + j\omega\varepsilon_s)\bar{\tilde{g}}^{y=0}_{z,l} \qquad \bar{\tilde{F}}^{y=W}_{sx,l} = -jk\frac{\mu_{a,y}}{\mu_{s,y}}\bar{\tilde{f}}^{y=W}_{ay,l} - (\sigma_{s,z} + j\omega\varepsilon_s)\bar{\tilde{g}}^{y=W}_{z,l} \tag{73}$$

where subscript s denotes the laminate material, a an ambient material. In FEA results, all field values can be taken from material s. In that case, Eqs. (72) and (73) are valid with subscript a replaced by subscript s. For $\mu_x = \mu_y$, Eqs. (3) and (7) give

$$\frac{\partial \bar{H}_{z1}}{\partial z} = -Q\left(\frac{\partial \bar{H}_{x1}}{\partial x} + \frac{\partial \bar{H}_{y1}}{\partial y}\right). \tag{74}$$

Equations (74), (22), (26), and the orthogonality of the eigenfunctions give

$$\bar{\tilde{F}}^{z=0}_{z,c,n} = Q\left(jk\bar{\tilde{f}}^{z=0}_{x,c,n} - K_n\bar{\tilde{f}}^{z=0}_{y,n}\right) \qquad \bar{\tilde{F}}^{z=T}_{z,c,n} = Q\left(jk\bar{\tilde{f}}^{z=T}_{x,c,n} - K_n\bar{\tilde{f}}^{z=T}_{y,n}\right) \tag{75}$$

where material subscripts have been skipped because of the continuity across the material interfaces.

2.2. A Laminate from 0 to Infinity in the Stacking Direction and Infinite in Other Directions

Figure 2 shows a cross section of an anisotropic, homogeneous approximation of a laminate with only one boundary.

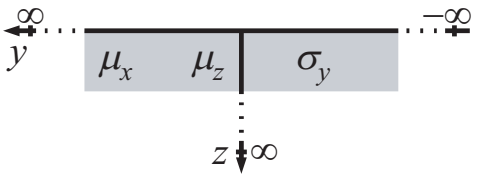

Figure 2. Cross section of an anisotropic approximation of a laminate with infinite extension in the y direction and extending from 0 to ∞ in the z direction. The only needed components of permeability and conductivity are μ_x, μ_z and σ_y.

The following simplifying constraints are added:

1. Neither $\bar{\mathbf{E}}$ nor $\bar{\mathbf{H}}$ depend on y.
2. H_y = constant.

Constraint 1 and 2 and Eqs. (5) and (6) imply that $\bar{E}_x = \bar{E}_z = 0$ and

$$\bar{E}_y = \frac{1}{\sigma_y + j\omega\varepsilon}\left(\frac{\partial \bar{H}_x}{\partial z} - \frac{\partial \bar{H}_z}{\partial x}\right) \tag{76}$$

Constraint 2, Eqs. (4) and (7) give

$$-j\omega\left(\hat{\boldsymbol{x}}\mu_x\bar{H}_x + \hat{\boldsymbol{z}}\mu_z\bar{H}_z\right) = -\hat{\boldsymbol{x}}\frac{\partial \bar{E}_y}{\partial z} + \hat{\boldsymbol{z}}\frac{\partial \bar{E}_y}{\partial x} \tag{77}$$

Constraint 2, Eqs. (3) and (7) give

$$\nabla\cdot\bar{\mathbf{B}} = \mu_x\frac{\partial \bar{H}_x}{\partial x} + \mu_z\frac{\partial \bar{H}_z}{\partial z} = 0 \tag{78}$$

Equations (76) and (78) inserted in Eq. (77) give the wave equation

$$Q\frac{\partial^2 \bar{H}_i}{\partial x^2} + \frac{\partial^2 \bar{H}_i}{\partial z^2} = \bar{\gamma}^2\bar{H}_i, \quad i = x \text{ or } z \tag{79}$$

2.2.1. Traveling Wave in x Direction

The periodic boundary conditions are (19). Dirichlet conditions, with $\bar{H}_z$ arbitrarily chosen to have phase angle 0 at $x = 0$, are

$$\bar{H}_x(x,0) = \widehat{H}_x e^{j(\varphi - kx)} \qquad \bar{H}_z(x,0) = \widehat{H}_z e^{-jkx}, \tag{80}$$

$$\bar{H}_i(x,\infty) \text{ is limited}, \quad i = x \text{ or } z. \tag{81}$$

Just as for plane waves [9], the wave equations for different components are independent and satisfied with any phase angle φ and amplitudes $\widehat{H}_x$ and $\widehat{H}_z$, but Faraday's law (77) imposes additional conditions that determine the phase differences and amplitude relationships of the electromagnetic field components as shown below. A Fourier series with terms of the form $\bar{\bar{Z}}_m(z)\bar{X}_m(x)$ inserted in Eq. (79) together with the orthogonality of the eigenfunctions $\bar{X}_m(x)$ give (32) without the y dependent term. The real part, a, and the imaginary part, b, of $\bar{\eta}^2$ are

$$a = Qk^2 - \omega^2 \varepsilon \mu_x \qquad b = \omega \mu_x \sigma_y. \tag{82}$$

The mathematical expressions of the real part, α, and the imaginary part, β, of $\bar{\eta}$ expressed in a and b are the same as in three dimensions and isotropic materials [7]. Since Eq. (81) requires $\bar{C}_{m,n}$ in Eq. (34) to be zero, and the conditions in Eq. (80) allow only the mode $m = -1$, the Fourier series of $\bar{H}_x$ and $\bar{H}_z$ contain only one term each and are given by

$$\bar{H}_x(x,z) = \widehat{H}_x e^{-\bar{\eta}z} e^{j(\varphi - kx)} \qquad \bar{H}_z(x,z) = \widehat{H}_z e^{-\bar{\eta}z} e^{-jkx}. \tag{83}$$

Equations (76) and (83) imply that $\bar{E}_y(x,z)$ can be expressed as

$$\bar{E}_y(x,z) = \widehat{E}_y e^{-\bar{\eta}z} e^{j(\phi - kx)}. \tag{84}$$

Since $\widehat{H}_x$, $\widehat{H}_z$ and $\widehat{E}_y$ are positive by definition, Eqs. (83), (84) and the z component of Eq. (77) imply that $\phi = 0$ and

$$\frac{\widehat{E}_y}{\widehat{H}_z} = \frac{\omega \mu_z}{k}. \tag{85}$$

Hence, $\bar{E}_y$ and $\bar{H}_z$ are in phase. This together with Eqs. (83), (84) and the x component of Eq. (77) give

$$\varphi = \theta + \frac{\pi}{2} \tag{86}$$

where $\theta = \arg \bar{\eta}$, and

$$\frac{\widehat{E}_y}{\widehat{H}_x} = \frac{\omega \mu_x}{\eta} = \frac{\omega \mu_x}{\left[(Qk^2 - \omega^2 \mu_x \epsilon)^2 + (\omega \mu_x \sigma_y)^2\right]^{1/4}}. \tag{87}$$

Equations (85) and (87) give

$$\frac{\widehat{H}_x}{\widehat{H}_z} = \frac{\mu_z \eta}{\mu_x k}. \tag{88}$$

Equations (84), (85), (87) and (69) with $\widehat{B}_x = \mu_x \widehat{H}_x$ and $\widehat{B}_z = \mu_z \widehat{H}_z$ give

$$p = \frac{\sigma_y}{2} \widehat{E}_y^2 e^{-2\alpha z} = \frac{\sigma_y \omega^2}{2\eta^2} \widehat{B}_x^2 e^{-2\alpha z} = 2\sigma_y \tau_p^2 f^2 \widehat{B}_z^2 e^{-2\alpha z} \tag{89}$$

where f is the electrical frequency, and τ_p is the pole pitch equal to $\lambda/2$.

2.2.2. Standing Wave in x Direction

The boundary conditions (19) and (81) are valid also in this case but (80) is replaced by the standing wave boundary conditions

$$\bar{H}_x(x,0) = \widehat{H}_x \frac{e^{j(kx-\varphi)} + e^{-j(kx-\varphi)}}{2} e^{j\Psi} \qquad \bar{H}_z(x,0) = \widehat{H}_z \frac{e^{jkx} + e^{-jkx}}{2}. \tag{90}$$

The solutions of Eq. (79) with boundary conditions contain the forward and backward going modes $m = -1$ and $m = 1$. The solutions are

$$\bar{H}_x(x,z) = \widehat{H}_x e^{j\Psi - \bar{\eta}z}\cos(kx-\varphi) \qquad \bar{H}_z(x,z) = \widehat{H}_z e^{-\bar{\eta}z}\cos kx. \tag{91}$$

Equations (76) and (91) give

$$\bar{E}_y(x,z) = \frac{e^{-\bar{\eta}z}}{\sigma_y + j\omega\epsilon}\left(-\bar{\eta}\widehat{H}_x e^{j\Psi}\cos(kx-\varphi) + k\widehat{H}_z \sin kx\right) \tag{92}$$

Also in this case Faraday's law, Eq. (77), imposes additional conditions that determine the phase differences and amplitude relationships of the electromagnetic field components. The x or z component of Eq. (77) implies that $\varphi = \pi/2$ since Eq. (77) is valid for any kx. With this and the x or z component of Eq. (77) $\widehat{H}_x e^{j\Psi}$ in Eq. (92) can be replaced by an expression with $\widehat{H}_z$. Therefore

$$\bar{E}_y(x,z) = \frac{e^{-\bar{\eta}z}}{\sigma_y + j\omega\epsilon}\left(-\bar{\eta}\widehat{H}_x e^{j\Psi} + k\widehat{H}_z\right)\sin kx = -j\frac{\omega\mu_z}{k}\widehat{H}_z e^{-\bar{\eta}z}\sin kx = \widehat{E}_y e^{-\bar{\eta}z}e^{j\Gamma}\sin kx \tag{93}$$

which with positive amplitudes implies that $\Gamma = -\pi/2$ and that the amplitude quotient $\widehat{E}_y/\widehat{H}_z$ is again given by Eq. (85). Hence, $\bar{E}_y$ is lagging $\bar{H}_z$ by $\pi/2$, and

$$\bar{E}_y(x,z) = -j\widehat{E}_y e^{-\bar{\eta}z}\sin kx. \tag{94}$$

The x or z component of Eq. (77) used for replacing $\widehat{H}_z$ by $\widehat{H}_x e^{j\Psi}$ in Eq. (93) gives

$$\bar{E}_y(x,z) = -j\frac{\omega\mu_x}{\bar{\eta}}\widehat{H}_x e^{j\Psi - \bar{\eta}z}\sin kx \tag{95}$$

which with positive amplitudes and Eq. (94) gives that the amplitude quotient $\widehat{E}_y/\widehat{H}_x$ is again given by Eq. (87), and

$$\Psi = \arctan\frac{\beta}{\alpha} = \theta. \tag{96}$$

Hence,

$$\bar{H}_x(x,z) = \widehat{H}_x e^{j\theta - \bar{\eta}z}\sin kx. \tag{97}$$

Equations (84), (87) and (85) with $\widehat{B}_z = \mu_z\widehat{H}_z$ give that the time average of the eddy current loss density is

$$p = \frac{\sigma_y}{2}\widehat{E}_y^2 e^{-2\alpha z}\sin^2 kx = 2\sigma_y\tau_p^2 f^2\widehat{B}_z^2 e^{-2\alpha z}\sin^2\frac{\pi x}{\tau_p}. \tag{98}$$

The only difference between (89) and (98) is the factor $\sin^2 kx$. The time averaged loss density in Eq. (98) averaged with respect to x is

$$p = \sigma_y\tau_p^2 f^2\widehat{B}_z^2 e^{-2\alpha z}. \tag{99}$$

A comparison between Eq. (89) and Eq. (99) shows that the average eddy current loss density in the case of a standing wave is half as large as in the case of a traveling wave.

2.3. A Laminate with Thickness $2T$ in the Stacking Direction and Infinite Extension in Other Directions

Figure 3 shows a cross section of an anisotropic approximation of laminate with thickness $2T$ and infinite extension in the y direction. A symmetry plane is assumed at $z = T$.

This case is a slight generalization of the case in Section 2.2.1. The laminate, that could be either the whole simplified stator core or just one simplified plate package, is assumed to be subjected to symmetrical magnetic field waves such that there is a symmetry plane half way through the thickness. Condition (81) is therefore replaced by

$$\frac{\partial\bar{H}_x(x,T)}{\partial z} = 0 \qquad \bar{H}_z(x,T) = 0. \tag{100}$$

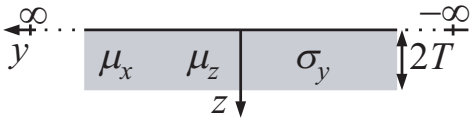

Figure 3. Cross section of an anisotropic approximation of a laminate from 0 to $2T$ in the z direction and infinite extension the other directions. The only needed permeability and conductivity components are μ_x, μ_z and σ_y.

Equation (34) multiplied by the only eigenfunction, e^{-jkx}, allowed by Eq. (80) gives

$$\bar{H}_x(x,z) = \left(\bar{C}_x e^{\bar{\eta}z} + \bar{D}_x e^{-\bar{\eta}z}\right) e^{-jkx} \qquad \bar{H}_z(x,z) = \left(\bar{C}_z e^{\bar{\eta}z} + \bar{D}_z e^{-\bar{\eta}z}\right) e^{-jkx}. \tag{101}$$

Equations (101), (80) and (100) give

$$\bar{C}_x = \frac{\widehat{H}_x e^{j\varphi-\bar{\eta}T}}{e^{\bar{\eta}T}+e^{-\bar{\eta}T}} \qquad \bar{D}_x = \frac{\widehat{H}_x e^{j\varphi+\bar{\eta}T}}{e^{\bar{\eta}T}+e^{-\bar{\eta}T}} \tag{102}$$

$$\bar{C}_z = -\frac{\widehat{H}_z e^{-\bar{\eta}T}}{e^{\bar{\eta}T}-e^{-\bar{\eta}T}} \qquad \bar{D}_z = \frac{\widehat{H}_z e^{\bar{\eta}T}}{e^{\bar{\eta}T}-e^{-\bar{\eta}T}}. \tag{103}$$

Equations (102) and (103) in Eq. (101) give

$$\bar{H}_x(x,z) = \widehat{H}_x e^{j(\varphi-kx)} \frac{\cosh\bar{\eta}(z-T)}{\cosh\bar{\eta}T} \tag{104}$$

$$\bar{H}_z(x,z) = \widehat{H}_z e^{-jkx} \frac{\sinh\bar{\eta}(T-z)}{\sinh\bar{\eta}T}. \tag{105}$$

Equations (76), (104) and (105) imply that $\bar{E}_y$ is

$$\bar{E}_y(x,z) = \frac{\sinh\bar{\eta}(z-T)e^{-jkx}}{\sigma_y+j\omega\varepsilon}\left(\frac{\widehat{H}_x\bar{\eta}e^{j\varphi}}{\cosh\bar{\eta}T} - \frac{jk\widehat{H}_z}{\sinh\bar{\eta}T}\right) = \widehat{E}_y \frac{\sinh\bar{\eta}(T-z)}{\sinh\bar{\eta}T} e^{j(\Phi-kx)} \tag{106}$$

where $\widehat{E}_y = |\bar{E}_y(x,0)|$, and Φ is an angle to determine such that it agrees with $\widehat{E}_y$ being a real positive number. The expression after the last equality sign in Eq. (106) is just a compact way of writing $\bar{E}_y(x,z)$ concluded from the other part of Eq. (106). Eqs. (105), (106) and the z component of Eq. (77) imply that $\Phi = 0$ and that the amplitude quotient $\widehat{E}_y/\widehat{H}_z$ is given by Eq. (85). The x component of Eq. (77) together with Eqs. (104) and (106) give

$$\frac{\widehat{E}_y}{\widehat{H}_x} = \frac{\omega\mu_x}{\eta}|\tanh\bar{\eta}T| e^{j(\varphi-\frac{\pi}{2}-\theta+\arg\tanh\bar{\eta}T)} = \frac{\omega\mu_x}{\eta}|\tanh\bar{\eta}T| = \frac{\omega\mu_x}{\eta}\sqrt{\frac{\cosh 2\alpha T-\cos 2\beta T}{\cosh 2\alpha T+\cos 2\beta T}} \tag{107}$$

where the second equality follows from the phase angle, φ, being determined such that the amplitude quotient is real and positive. Hence the exponent is zero, and

$$\varphi = \theta + \frac{\pi}{2} - \arg\tanh\bar{\eta}T = \theta + \frac{\pi}{2} - \arctan\frac{\sin 2\beta T}{\sinh 2\alpha T}. \tag{108}$$

Equations (85) and (87) give

$$\frac{\widehat{H}_x}{\widehat{H}_z} = \frac{\frac{\widehat{E}_y}{\widehat{H}_z}}{\frac{\widehat{E}_y}{\widehat{H}_x}} = \frac{\mu_z\eta}{\mu_x k|\tanh\bar{\eta}T|} = \frac{\mu_z\eta}{\mu_x k}\sqrt{\frac{\cosh 2\alpha T+\cos 2\beta T}{\cosh 2\alpha T-\cos 2\beta T}} \tag{109}$$

The quotients $\widehat{H}_x/\widehat{H}_z$, $\widehat{E}_y/\widehat{H}_x$ and the angle φ approach the values in Section 2.2.1 when T approaches ∞. Eqs. (85), (69) and (106) with $\Phi = 0$ and $\widehat{B}_z = \mu_z\widehat{H}_z$ give

$$p = \frac{\sigma_y}{2}\widehat{E}_y^2\chi(z,T) = 2\sigma_y\tau_p^2 f^2\widehat{B}_z^2\chi(z,T) \tag{110}$$

where

$$\chi(z,T) = \frac{\cosh 2\alpha(z-T)-\cos 2\beta(z-T)}{\cosh 2\alpha T-\cos 2\beta T} \to e^{-2\alpha z} \text{ when } T\to\infty. \tag{111}$$

3. COMPARISONS BETWEEN FOURIER SERIES AND FEA FOR THE LAMINATE OF WIDTH W AND THICKNESS T

The methods of comparisons are mainly the same as for isotropic materials [7], but in the anisotropic 3-D cases sine interpolation has been used because of difficulties encountered with the accuracy of $\bar{\mathbf{E}}$. Fig. 4 shows the FE model except the air or vacuum that is assumed to enclose the laminate with thickness 10 mm in the z direction and width 30 mm in the y direction. The model spans 90 mm, which is one half wave length, in the x direction. The air gap is 12 mm from the primary magnetic field source to the laminate. The primary source has 18 current bars with amplitude 100 A and 10° phase difference from one bar to the next.

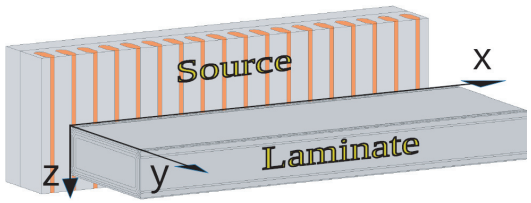

Figure 4. FE model of the geometry of a laminate and a primary magnetic field source.

The laminate is assumed to have stacking factor $k = 0.95$ and to consist of varnish insulated sheets of cold worked stainless steel 201 L with thickness $t_s = 0.5$ mm, conductivity 1.5 MS/m and relative permeability $\mu_{r,s} = 36$ [10]. These data give varnish thickness $t_v = t_s/k - t_s$. In directions tangential to the sheet planes, the effective permeance can be defined as the sum of the permeances of the layers of steel and varnish. This gives the effective relative laminate permeability $\mu_{r,xy} = (\mu_{r,s}t_s + \mu_{r,v}t_v)/(t_s + t_v) = 34.25$ in the tangential directions if the relative permeability of the varnish is $\mu_{r,v} = 1$. The effective reluctance in the stacking direction can be defined as the sum of the reluctances of the layers of steel and varnish. This gives the effective relative laminate permeability $\mu_{r,z} = (t_s + t_v)/(t_s/\mu_{r,s} + t_v/\mu_{r,v}) \approx 13.09$ in the stacking direction [2]. The relative permeability in the source core is 8000. An effective conductivity calculated similarly to $\mu_{r,xy}$ could have been used, but the conductivity parallel to the laminate planes was simply chosen to be 1.5 MS/m. The conductivity σ_z was chosen to be 2 S/m which is low enough to satisfy $\sigma_z \ll \sigma_x$ and high enough to give a not too noisy $\bar{E}_z$ with the used mesh. According to FEA, $\bar{E}_z$ changes more abruptly near $z = 0$ and T the lower σ_z is. This abrupt change requires a fine mesh at the surface for accurate calculation of $\bar{E}_z$ there. On the other hand, this is not important for the eddy current losses since $J_z \ll J$ if σ_z is small enough to make $\bar{E}_z$ noisy. The boundary values were taken from the FE model, inside the laminate, 100 nm from the boundaries at $z = 0$ and T, and at $y = 0.8$ mm instead of $y = 0$, and from $y = 29.2$ mm instead of $y = 30$ mm because of the bad accuracy of the FEA closest to the edges of the magnetic plate. Therefore, $W = 28.4$ mm in the analytical expressions. Finite elements of higher order than default were used to get smoother $\bar{\mathbf{E}}$. The amplitudes of components of $\bar{\mathbf{H}}$ and $\bar{\mathbf{E}}$ along selected lines in the plates are shown in Figs. 5 and 6 respectively. The values of $\bar{E}_y$, especially close to $z = 0$ and T, are not so accurate because of numerical cancellation between the about 30 times larger $\bar{E}_{y\eta}$ and $\bar{E}_{y\nu}$. A remedy for this is to replace the $\bar{E}_{y\nu}$ values closest to $z = 0$ and T by $\bar{E}_{y\nu}$ values interpolated and extrapolated from internal points along the same line of evaluation. Fig. 6 shows results where this has been done. Another way is to use higher accuracy in the determination of the boundary functions, but that has hardly been possible with ANSYS and the used computer. The lines of evaluation of results have been chosen to be not so close to any boundary, so that the results are completely dominated by the values at a single boundary. The time averaged eddy current loss density along the evaluation lines is shown in Fig. 7.

4. DISCUSSION

If a field component expressed as a sine Fourier series is not zero where all the eigenfunctions are zero, the sine series suffer from bad accuracy because of the Gibbs phenomenon, but this can be avoided by

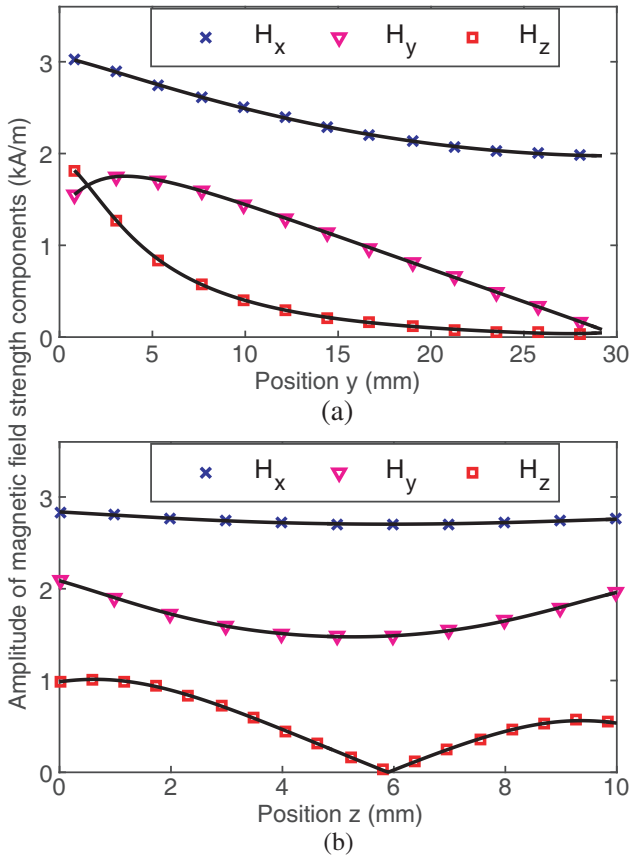

Figure 5. Amplitudes of components of magnetic field strength versus (a) y at $z = 2\,\text{mm}$, and (b) z at $y = 5\,\text{mm}$. The continuous curves show the values of Fourier series. The discrete plot symbols show FEA results.

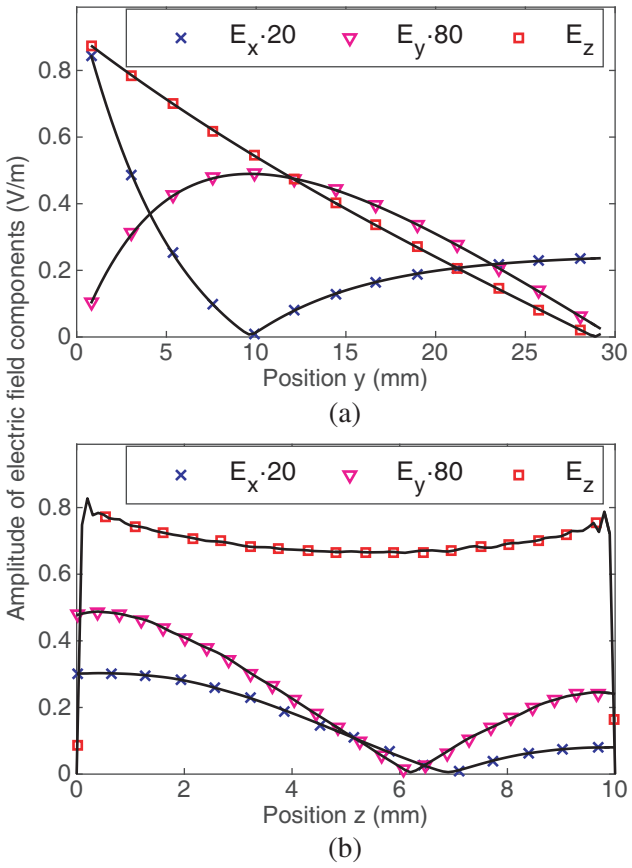

Figure 6. Amplitudes of components of electric field strength versus (a) y at $z = 2\,\text{mm}$, and (b) z at $y = 5\,\text{mm}$. The continuous curves show the values of Fourier series. The discrete plot symbols show FEA results.

sine interpolation. Trigonometric interpolation coefficients can be calculated with the discrete Fourier transform if the eigenfunctions are of the exponential form suitable for periodic signals [11, 12]. However, the eigenfunctions depending on y and z in this article are either sine or cosine functions because of the boundary conditions. For a function approximated by a truncated sine Fourier series containing the n first modes, the truncated series interpolates the function in n equidistant, internal points if the Fourier coefficients are approximated by use of the trapezoidal rule. A proof of this is given in appendix. A truncated cosine series with Fourier coefficients approximated with the trapezoidal rule does not interpolate the function and, according to FEA, does not in general give better accuracy than a truncated cosine series with Fourier coefficients calculated with almost exact integration. For cosine series, the trapezoidal rule is still a good choice because it allows a high speed of calculation compared to almost exact integration with the integral function in MATLAB.

In the 2-D cases, treated in Sections 2.2 and 2.3, the conductivity in the stacking direction does not matter, and the expressions for fields and loss density are relatively simple. The 2-D case expressions predict fields that decrease exponentially into the material. This can only be approximately true in laminates with finite width and thickness. One reason for that is that the boundaries and the fields on these give rise to field modes that can give local maxima of field components and eddy current loss density, as demonstrated by the results in Section 3. Real electric machines have finite size, but the last expression in Eq. (89) seems to indicate that a machine with a large α and a small τ_p is desirable for making the eddy current losses low. Decreasing τ_p affects α very little until τ_p becomes very small so that $a \gg b$. For a given machine size it may therefore be advantageous to have many poles if it is

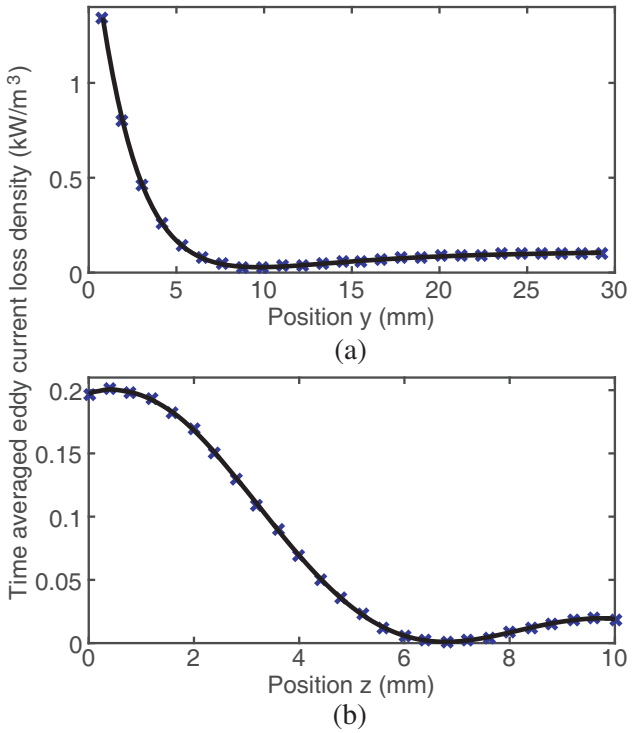

Figure 7. Time average of eddy current loss density versus (a) y at $z = 2\,\text{mm}$, and (b) z at $y = 5\,\text{mm}$. The continuous curves show the values of Fourier series. The discrete plot symbols show FEA results.

important to keep the eddy current losses low in the core. A simple estimation with a homogeneous $\bar{B}_z$ indicates that this could be true also for a conventional synchronous machine for the same reason that lamination reduces eddy current loss, i.e., the combined loss caused by n small eddies is smaller than the loss caused by one large eddy. The reason for this is that the eddy current density is roughly proportional to the eddy radius, and the loss density is proportional to the square of the eddy current density. However, other losses, such as, e.g., those caused by hysteresis, friction, and resistance in windings will also, in general, be affected by an increased number of poles.

5. CONCLUSIONS

The derived mathematical expressions make it possible to calculate spatially smoothed out, time harmonic, traveling electric and magnetic fields within a laminate from measured or calculated field values on the boundaries of the laminate. With the z direction as the stacking direction, and the material isotropic in the directions perpendicular to the stacking direction, the spatially smoothed $\bar{H}_z$ can be determined from the wave equation with boundary conditions. With this $\bar{H}_z$ used as a source term in 2-D Poisson equations with boundary conditions, it is possible to estimate the other magnetic and the electric field components in a laminate approximated by a homogeneous, anisotropic block if the conductivity in the z direction is negligible. Sufficient conditions for the complete determination of the spatially smoothed electric and magnetic field within the laminate are knowledge of 1: the values of $\bar{\mathbf{H}}$ on the end planes at constant z, and 2: three of the six Cartesian components of the magnetic and electric field on each boundary surface perpendicular to the lamination planes. These three components that must be known on the latter boundary surfaces depend on the choice of combination of Neumann and Dirichlet boundary conditions. Without knowledge of $\bar{H}_x$ and $\bar{H}_y$ at the end planes at constant z, excellent $\bar{\mathbf{H}}$ field agreement between Fourier series and FEA is still possible. However, in that case, the differential equations with Dirichlet and Neumann conditions imply that the $\bar{\nu}$ dependent Fourier series of $\bar{E}_x$ and $\bar{E}_y$ become sine series that are discontinuous at the end planes at constant z. The discontinuities lead to the Gibbs phenomenon and therefore lower accuracy. The accuracy can be

increased with sine interpolation.

The average eddy current loss density during a cycle in an infinite laminate with one boundary plane parallel to the laminate sheets is proportional to the square of the product of the longitudinal wave length, the frequency and the amplitude of the normal component of the magnetic flux density. In this case, the spatial average of the eddy current loss density is twice as large for a traveling wave as for a standing wave.

ACKNOWLEDGMENT

The research presented in this thesis was carried out as a part of "Swedish Hydropower Centre — SVC". SVC has been established by the Swedish Energy Agency, Elforsk and Svenska Kraftnät together with Luleå University of Technology, The Royal Institute of Technology, Chalmers University of Technology and Uppsala University.

APPENDIX A. THEOREM OF INTERPOLATION BY A TRUNCATED SINE FOURIER SERIES

Theorem: A truncated sine Fourier series, $g(x)$, that approximates a function, $f(x)$, at $x \in [0, c]$ interpolates f in n internal points if the following conditions are satisfied:
1. $g(x)$ contains the n first modes.
2. $g(0) = g(c) = 0$.
3. The Fourier coefficients are approximated by use of the trapezoidal rule.
4. The $n + 2$ points, including the two end points, are equidistant.

Proof: Conditions 1 and 2 give

$$g(x) = \sum_{\nu=1}^{n} a_\nu \sin \nu \frac{\pi}{c} x \tag{A1}$$

where the Fourier coefficient according to conditions 3 and 4 is given by

$$a_\nu = \frac{2}{n+1} \sum_{i=1}^{n} f_i \sin \nu \frac{i\pi}{n+1}. \tag{A2}$$

With the Fourier coefficients collected in a vector, Eq. (A2) can be expressed as

$$\mathbf{a} = \boldsymbol{\mathcal{A}}\mathbf{f} \tag{A3}$$

where

$$\mathbf{a} = \begin{bmatrix} a_1 \\ \vdots \\ a_n \end{bmatrix}, \qquad \boldsymbol{\mathcal{A}} = \frac{2}{n+1} \begin{bmatrix} \sin \frac{\pi}{n+1} & \dots & \sin \frac{n\pi}{n+1} \\ \vdots & \ddots & \vdots \\ \sin \frac{n\pi}{n+1} & \dots & \sin \frac{n^2\pi}{n+1} \end{bmatrix}, \qquad \mathbf{f} = \begin{bmatrix} f_1 \\ \vdots \\ f_n \end{bmatrix}. \tag{A4}$$

A function $h(x)$ of the same form as $g(x)$ is

$$h(x) = \sum_{\nu=1}^{n} b_\nu \sin \nu \frac{\pi}{c} x. \tag{A5}$$

The requirement that h must interpolate f in n points leads to the equation system $\mathbf{Ab} = \mathbf{f}$ with solution

$$\mathbf{b} = \mathbf{A}^{-1}\mathbf{f} \tag{A6}$$

where

$$\mathbf{A} = \begin{bmatrix} \sin \frac{\pi}{n+1} & \dots & \sin \frac{n\pi}{n+1} \\ \vdots & \ddots & \vdots \\ \sin \frac{n\pi}{n+1} & \dots & \sin \frac{n^2\pi}{n+1} \end{bmatrix}, \qquad \mathbf{b} = \begin{bmatrix} b_1 \\ \vdots \\ b_n \end{bmatrix}. \tag{A7}$$

A comparison between Eqs. (A3) and (A6) gives that $\mathbf{b} = \mathbf{a}$ if $\mathbf{A^{-1}} = \mathcal{A}$, or, equivalently, $\mathbf{A}\mathcal{A} = \mathbf{I}$ where $\mathbf{I}$ is the identity matrix. With $\delta = \frac{(i-k)\pi}{n+1}$, and $\sigma = \frac{(i+k)\pi}{n+1}$, an arbitrary element in $\mathbf{A}\mathcal{A}$ is

$$(\mathbf{A}\mathcal{A})_{i,k} = \frac{2}{n+1}\sum_{p=1}^{n} \sin k\frac{p\pi}{n+1}\sin p\frac{i\pi}{n+1} = \frac{1}{n+1}\mathcal{R}e\left\{\sum_{p=1}^{n}\left(e^{jp\delta} - e^{jp\sigma}\right)\right\} = s_\delta - s_\sigma \tag{A8}$$

where s_δ and s_σ are geometric sums. For $i \neq k$,

$$s_\delta = \frac{1}{n+1}\mathcal{R}e\left\{\frac{(e^{j\delta})^{n+1} - e^{j\delta}}{e^{j\delta}-1}\right\} = \frac{1}{n+1}\mathcal{R}e\left\{\frac{((-1)^{i-k} - e^{j\delta})(e^{-j\delta}-1)}{(e^{j\delta}-1)(e^{-j\delta}-1)}\right\} = -\frac{1+(-1)^{i-k}}{2(n+1)}. \tag{A9}$$

For all i and k,

$$s_\sigma = \frac{1}{n+1}\mathcal{R}e\left\{\frac{(e^{j\sigma})^{n+1} - e^{j\sigma}}{e^{j\sigma}-1}\right\} = -\frac{1+(-1)^{i+k}}{2(n+1)} = -\frac{1+(-1)^{i-k}}{2(n+1)}. \tag{A10}$$

Equations (A8), (A9) and (A10) give $(\mathbf{A}\mathcal{A})_{i,k} = 0$ for $i \neq k$. For $i = k$, Eq. (A8) gives that $s_\delta = \frac{n}{n+1}$ which together with Eq. (A10) gives $(\mathbf{A}\mathcal{A})_{i,i} = \frac{n}{n+1} + \frac{1}{n+1} = 1$. Hence, $\mathbf{b} = \mathbf{a}$, and the approximation, g, of a truncated Fourier series interpolates the function f. This concludes the proof.

REFERENCES

1. Cheng, L., S. Sudo, Y. Gao, H. Dozono, and K. Muramatsu, "Homogenization technique of laminated core taking account of eddy currents under rotational flux without edge effect," *IEEE Transactions on Magnetics*, Vol. 49, No. 5, 1969–1972, May 2013.
2. Reece, A. B. J. and T. W. Preston, *Finite Element Methods in Electrical Power Engineering*, Oxford University Press, 2000.
3. Lin, D., P. Zhou, Z. Badics, W. Fu, Q. Chen, and Z. Cendes, "A new nonlinear anisotropic model for soft magnetic materials," *IEEE Transactions on Magnetics*, Vol. 42, No. 4, 963–966, Apr. 2006.
4. Bermudez, A., D. Gomez, and P. Salgado, "Eddy-current losses in laminated cores and the computation of an equivalent conductivity," *IEEE Transactions on Magnetics*, Vol. 44, No. 12, 4730–4738, Dec. 2008.
5. Lin, R., A. Haavisto, and A. Arkkio, "Axial flux and eddy-current loss in active region of a large-sized squirrel-cage induction motor," *IEEE Transactions on Magnetics*, Vol. 46, No. 11, 3933–3938, Nov. 2010.
6. Marcusson, B. and U. Lundin, "Axial magnetic fields, axial force, and losses in the stator core and clamping structure of a synchronous generator with axially displaced stator," *Electric Power Components and Systems*, Vol. 45, No. 4, 410–419, 2017, [Online], Available: http://dx.doi.org/10.1080/15325008.2016.1266062.
7. Marcusson, B. and U. Lundin, "Harmonically time varying, traveling electromagnetic fields along a plate and a laminate with a rectangular cross section, isotropic materials and infinite length," *Progress In Electromagnetics Research B*, Vol. 77, 117–136, 2017.
8. Brander, O., "Partiella Differentialekvationer-en kurs i fysikens matematiska metoder, del B," Studentlitteratur, 1973.
9. Griffiths, D. J., *Introduction to Electrodynamics*, 3rd Edition, Pearson, Addison Wesley, 1999.
10. "Matweb website," http://matweb.com/search/AdvancedSearch.aspx, accessed Feb. 16, 2017.
11. "Trigonometric interpolation," [Online], Available: http://www.math.vt.edu/people/embree/math5466/lecture7.pdf.
12. "Trigonometric interpolation and the fft," [Online], Available: http://math.gmu.edu/ tsauer/na/ch10.pdf.